Fundamental Limits for Linearity of CATV Lasers

V. B. Gorfinkel and S. Luryi, *Fellow, IEEE*

***Abstract*—We have considered nonlinear distortions in a subcarrier multiplexed optical transmission system arising from carrier heating effects in the source laser. We included two sources of carrier heating: free-carrier absorption of the coherent radiation in the cavity, and the power flux into the active layer, associated with the input current. Resulting from the very existence of modulated optical and electrical signals, these effects cannot be avoided in any laser structure. Simple analytic expressions have been derived for the intermodulation distortion in multichannel single-mode lasers. For an 80-channel 60–540 MHz system with 3% optical modulation depth per channel, the composite second-order (CSO) distortion brought about by the hot-carrier effects is near the tolerance limit for CATV systems.**

I. Introduction

SUBCARRIER multiplexed (SCM) optical transmission systems, such as cable television (CATV) networks, require low-distortion distributed feedback (DFB) lasers. The amplitude modulation (AM) frequency division multiplexing (FDM) scheme is the preferred SCM technique in CATV networks, mostly because of its compatibility with conventional electrical transmission systems. The AM-FDM scheme presents severe requirements to the linearity of the transmission. Typically, the composite second-order distortion must not exceed −60 dBc. Channel capacity in current systems is about 40 channels, but future CATV networks are expected to carry much larger number of channels [1]. Linearity specifications for an 80–100 channel system become extremely stringent.

The dominant intermodulation distortion (IMD) is commonly attributed to the nonlinearity of the light-current characteristics arising from a spatially inhomogeneous distribution of the optical field. Other sources of nonlinearity, such as the leakage current and the intrinsic (resonance) distortion, are considered relatively small [2]. However, inhomogeneous field distribution is not fundamentally inherent to DFB lasers. Thus, lasers with a practically homogeneous field distribution have been obtained [3] by introducing two $\lambda/8$ phase shifts in the DFB grating. It is therefore reasonable to discuss *fundamental* limitations to the linearity of analog lasers without the spatial hole burning.

Two fundamental sources of nonlinearity have been discussed in the literature: the intrinsic (resonance) distortion [4] and the clipping of the multiplex signal at the laser threshold [5]. The clipping distortion has been extensively studied [6]–[9] and accurate formulas are available. As to the intrinsic distortion, it is sometimes claimed to be small in the CATV frequency range ($\lesssim$ 600 MHz). That claim, however, must be qualified: since the intrinsic IMD decreases with the increasing resonance frequency f_r of the laser as $(f/f_r)^2$ [4], it becomes small only at sufficiently high bias currents. However, increasing the steady-state bias introduces additional nonlinearities that account for the observed minimum in the dependence of the CSO on the bias current (see, for example, Kawamura *et al.* [10] who considered a phenomenological threshold gain term in the rate equations that varies under modulation). Whether or not the intrinsic distortion is "small" depends on the position of the minimum, and therefore on the nature of the additional nonlinearity.

Presently, we consider another fundamental nonlinearity, arising from the *free-carrier absorption* of the coherent radiation in the laser cavity. Although by itself this effect is linear, it becomes a source of nonlinearity when one takes into account the *carrier heating* by the coherent radiation and the input current. Resulting from the very existence of a modulated optical signal, these effects cannot be avoided in any laser structure. Extending the standard model of laser dynamics to take into account the carrier heating effect, we derive simple analytic expressions both for the static nonlinearity of the light-current characteristics and for the CSO distortion in an arbitrary AM-FDM SCM system with any (not necessarily random) distribution of carrier phases. For an exemplary random-phase 80 channel 540 MHz system, based on a 1.5 μm InGaAsP DFB laser, we show that these fundamental nonlinearities alone, even without the inclusion of clipping, account for an IMD near the limit of acceptable.

II. Model

We describe the laser by the standard system of rate equations for carrier(n) and photon (S) densities in the active layer, combined with an energy balance equation for carriers:

$$\frac{dn}{dt} = J - gS - \frac{n}{\tau_{\rm sp}} \tag{1a}$$

$$\frac{dS}{dt} = \Gamma S(g - \alpha n) - \frac{S}{\tau_{\rm ph}} \tag{1b}$$

$$\frac{3}{2}\frac{dT_e}{dt} = \frac{\alpha S\hbar\Omega}{2} + \frac{J\Delta}{2n} - \frac{3}{2}\frac{T_e - T}{\tau_\varepsilon} \tag{1c}$$

where $J \equiv I/eV_a$ is the electron flux per unit volume V_a of the active layer, I the pumping current, g the optical gain in the active layer, Ω the optical frequency, Γ the confinement factor for the radiation intensity, $\tau_{\rm sp}$ the lifetime of carriers (including nonradiative), $\tau_{\rm ph}$ the photon lifetime in the cavity, T_e the

Manuscript received August 23, 1994.

V. B. Gorfinkel is with the Department of High Frequency Engineering, University of Kassel, D-34121, Germany.

S. Luryi was with AT&T Bell Laboratories, Murray Hill, NJ 07974 USA. He is now with the Department of Electrical Engineering, State University of New York at Stony Brook, Stony Brook, NY 11794-2350 USA.

IEEE Log Number 9406445.

TABLE I
ASSUMED PARAMETERS (MULTIPLE QW LASER)

Symbol	Value	Comment
$\hbar\Omega$	0.8 eV	$\lambda = 1.55$ μm
(m_e, m_h)	$(0.041, 0.5)m_0$	(electron, hole) eff. mass
g_{max}	$4.0 \cdot 10^3$ cm^{-1}	Eq. (2)
d_{QW}	70 Å	7 wells
V_a	12.25 μm^3	250×1×0.05
Γ	0.04	confinement factor
Δ	300 meV	$(\Delta E_G)_{eff}$
α	$0.19 \cdot 10^{-6}$ cm^3/s	$\alpha_0 = 25$ cm^{-1} at $p = 10^{18}$ cm^{-3}
$\bar{c}$	$0.75 \cdot 10^{10}$ cm/s	$\bar{c} = c/\kappa_g$, $\kappa_g = 4$
τ_{ph}	3.34 ps	photon lifetime
τ_{sp}	0.5 ns	carrier lifetime
τ_ε	2 ps	energy relaxation time
P	$\eta V_a \hbar\Omega S/\Gamma\tau_{ph}$	output optical power
η	0.5	$S \rightarrow P$ efficiency
$R_{I:J}$	$1.96 \cdot 10^{-27}$ mA·cm^3·s	$I:J$ ratio
$R_{P:S}$	$5.88 \cdot 10^{-15}$ mW·cm^3	$P:S$ ratio

carrier temperature in energy units, τ_ε the energy relaxation time, $\alpha > 0$ is the free carrier absorption rate, and Δ is the kinetic energy per carrier injected into the active region. It is assumed in (1c) that effectively only one type of carriers absorbs radiation and that the number of electrons and holes is the same in the active layer, $n = p$, hence the factor of 2.

For the free-carrier absorption coefficient, Henry *et al.* [11] cite$\alpha_0 = 25$ cm^{-1} at $p = 10^{18}$ cm^{-3} and $\lambda = 1.6$ μm. Our α is related to α_0 by $\alpha_0 = \alpha p\bar{c}$, where $\bar{c} \equiv c/\kappa_g$ is the group velocity. The energy Δ depends on the laser structure, e.g., the fraction of carriers that get into the active region by tunneling; in general, we can say that $\Delta \lesssim \Delta E_G$, where ΔE_G is the bandgap difference between the cladding and the active layers. For InP cladding ($E_G = 1.35$ eV) and 1.55 μm active layer, $\Delta E_G = 0.55$ eV; we take a conservative estimate $\Delta = 0.3$ eV. For the energy relaxation time, we take $\tau_\varepsilon = 2$ ps. At higher carrier concentrations, one can expect even longer τ_ε because of the optical phonon bottleneck. Our assumed values of Δ and τ_ε result in a steady-state overheating of $T_e - T \approx 4$ K at the laser threshold, which is quite modest compared to calculations (see, e.g., [12]) that include the bottleneck effect. Experimental estimates for τ_ε vary widely; recently Hall *et al.* [13] found a time constant of ~ 1 ps in strained-layer quantum well (QW) 1.5 μm laser amplifiers. Sensitivity of our results to the assumed value of τ_ε is discussed in Section VI.

We assume that the carrier ensembles are at all times described by a quasi-equilibrium distribution, parameterized by the effective temperature T_e, which we moreover assume to be the same for both electrons and holes. Validity of this approximation relies on the rapidity of the electron-electron and electron-hole scattering rates, compared to all other characteristic times in the problem, including energy relaxation. The gain function g is then of the form

$$g(T_e, n, \Omega) = g_{\max}(f_e + f_h - 1) \tag{2}$$

where f_e and f_h are the Fermi functions of electrons and holes, respectively, at energies selected by the incident photons $\hbar\Omega$.

We consider a multiple QW laser with the radiative transition between the heavy-hole and the lowest electron subbands near the fundamental absorption edge. In this case,

$$f_e(n_S, T_e) = 1 - e^{-\pi\hbar^2 n_S/m_e T_e} \tag{3a}$$

$$f_h(n_S, T_e) = 1 - e^{-\pi\hbar^2 n_S/m_h T_e} \tag{3b}$$

where m_e and m_h are, respectively, the effective masses of electron and holes, and $n_s = nd_{\mathrm{QW}}$ is the sheet carrier concentration in the QW. Assumed parameters of the laser at $T = 300$ K are listed in Table I.

The values of n and T_e corresponding to the situation when the laser is pumped to transparency ($g = 0$) will be denoted by n_X and T_{eX}. Even though the lightwave intensity is negligible below threshold, $S = 0$, there is some carrier heating due to the current $J_X = n_X/\tau_{\mathrm{sp}}$. The values of n_X, T_{eX}, and J_X are determined by the equations

$$T_{eX} - T = \frac{\tau_\varepsilon \Delta}{3\tau_{\mathrm{sp}}} \tag{4a}$$

$$f_e + f_h = 1. \tag{4b}$$

Away from transparency, we can write approximately

$$g = g'_T(T_e - T_{eX}) + g'_n(n - n_X) \tag{5}$$

where the coefficients are readily determined from (2)–(4)

$$g'_n(T_{eX}, n_X) \equiv \left[\frac{\partial g}{\partial n}\right]_{n_X, T_{eX}} = \frac{\pi\hbar^2 d_{\mathrm{QW}}}{T_{eX}}\left(\frac{f_h}{m_e} + \frac{f_e}{m_h}\right) g_{\max} \tag{6a}$$

$$g'_T(T_{eX}, n_X) \equiv \left[\frac{\partial g}{\partial T_e}\right]_{n_X, T_{eX}} = -(n_X/T_{eX})g'_n. \tag{6b}$$

Fig. 1 compares the linear approximation (5) to the exact expression, (2).

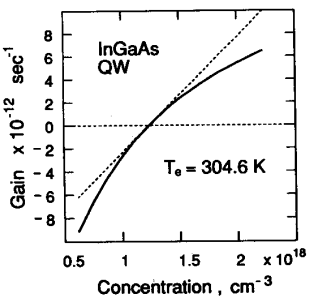

(a)

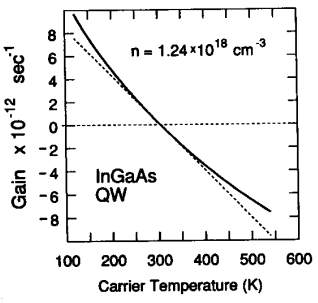

(b)

Fig. 1. Gain function $g(T_e, n)$ calculated from (2) and (3)for fixed values of (a) T_e and (b) n. Dotted lines correspond to the linear approximation, (5) with the parameters $T_{eX} = 304.6$ K,$n_x = 1.24 \cdot 10^{18}$ cm^{-3}, $g'_n = 1.01 \cdot 10^{-5}$ cm^3/s, and $g'_T = -4.75 \cdot 10^{11}$ meV$^{-1} \cdot$ s^{-1}.

We shall denote the stationary variables by a bar, viz. $\overline{S}$, $\overline{J}$, $\overline{n}$, etc., From (1) we have

$$\overline{J} = \overline{g}\overline{S} + \frac{\overline{n}}{\tau_{sp}} \tag{7a}$$

$$\overline{g} = \alpha\overline{n} + \frac{1}{\Gamma\tau_{ph}} \tag{7b}$$

$$\overline{T}_e = T + \gamma_S\overline{S} + \gamma_J\overline{J} \tag{7c}$$

where

$$\gamma_S \equiv \frac{1}{3}\alpha\tau_\varepsilon\hbar\Omega \qquad \gamma_J \equiv \frac{1}{3\overline{n}}\tau_\varepsilon\Delta. \tag{8}$$

Threshold values of T_e and n are determined by letting $\overline{S} = 0$ in (7)

$$g(T_{th}, n_{th}) = \alpha n_{th} + 1/\Gamma\tau_{ph} \tag{9a}$$

$$T_{th} - T = \frac{\gamma_J n_{th}}{\tau_{sp}} = \frac{\tau_\varepsilon\Delta}{3\tau_{sp}}. \tag{9b}$$

The subscript "th" denotes threshold values, e.g., $g_{th} \equiv g(T_{th}, n_{th})$. Comparing (4a) and (9b), we see that $T_{th} = T_{eX}$. The value of n_{th} must be found by solving the transcendental equation (9a). An estimate can be made with the help of the linear approximation (5). Substituting $g_{th} = g'_n(n_{th} - n_X)$ in (9a), we have

$$n_{th} \approx \frac{1/\Gamma\tau_{ph} + g'_n n_X}{g'_n - \alpha}. \tag{10}$$

It is evident from Fig. 1(a) that (10) underestimates n_{th} (in fact, quite severely for small values of $\Gamma\tau_{ph}$). This is particularly obvious if we neglect the free carrier absorption so that the threshold is achieved when g rises to match the constant loss $(\Gamma\tau_{ph})^{-1}$ at the mirrors. Clearly, the linear approximation reaches the same level at a lower value of n than does the concave exact curve.

III. Static Characteristics

Denoting by $\Delta\overline{X}$ the steady-state value of a variable X relative to its threshold value, viz. $\Delta\overline{X} \equiv \overline{X} - X_{th}$, let us rewrite (5) in the form

$$g = g_{th} + g'_T\,\Delta\overline{T}_e + g'_n\,\Delta\overline{n} \tag{11}$$

where the parameters g'_n and g'_T are defined at the threshold

$$g'_n \equiv \left[\frac{\partial g}{\partial n}\right]_{n_{th}, T_{th}} = \frac{\pi\hbar^2 d_{QW}}{T_{th}}\left(\frac{1-f_e(n_{th})}{m_e} + \frac{1-f_h(n_{th})}{m_h}\right) g_{max} \tag{12a}$$

$$g'_T \equiv \left[\frac{\partial g}{\partial T_e}\right]_{n_{th}, T_{th}} = -(n_{th}/T_{th})g'_n. \tag{12b}$$

Note the difference between (12a) and (6a), arising since at threshold the transparency equation (4b) no longer holds.

Variations δT_e and δn (not necessarily small) between any two steady states are related. Indeed, (7) is valid for any steady state; varying (7b) we find that the variations $\Delta\overline{T}_e$ and $\Delta\overline{n}$ are related as follows:

$$\Delta\overline{n} = -\frac{g'_T\,\Delta\overline{T}_e}{g'_n - \alpha} = -\frac{g'_T(\gamma_S\,\Delta\overline{S} + \gamma_J\,\Delta\overline{J})}{g'_n - \alpha} \equiv \tau_J\,\Delta\overline{J} + \tau_S g_{th}\overline{S} \tag{13}$$

where

$$\Delta\overline{J} \equiv \overline{J} - J_{th}; \qquad \Delta\overline{S} = \overline{S};$$

$$\Delta\overline{T}_e \equiv \overline{T}_e - T_{th}; \qquad \Delta\overline{n} \equiv \overline{n} - n_{th}; \tag{14}$$

and

$$\tau_J \equiv -\frac{g'_T\gamma_J}{g'_n - \alpha} \approx \frac{\tau_\varepsilon \cdot \Delta}{3T_{th}};$$

$$\tau_S \equiv -\frac{g'_T\gamma_S}{g_{th}(g'_n - \alpha)} \approx \frac{\alpha n_{th}}{g_{th}}\frac{\tau_\varepsilon \cdot \hbar\Omega}{3T_{th}}. \tag{15}$$

Substituting (14) in (7a) and using (11) and (13), we obtain the following expression for the nonlinear light-current characteristic:

$$\Delta\overline{J}(1 - \tau_J/\tau_{sp}) = \overline{S}g_{th}(1 + \tau_S/\tau_{sp}) + \overline{S}^2\alpha g_{th}\tau_S + \overline{S}\,\Delta\overline{J}\alpha\tau_J. \tag{16}$$

The slope efficiency is found by differentiating (16), giving

$$\frac{d\overline{S}}{d\overline{J}} = \frac{1}{g_{th}}\frac{1 - \tau_J/\tau_{sp} - \tau_J\alpha\overline{S}}{1 + \tau_S/\tau_{sp} + 2\tau_S\alpha\overline{S} + \tau_J(\alpha/g_{th})\,\Delta\overline{J}} \approx \frac{1 - \xi_0\overline{S}}{g_{th}} \tag{17}$$

TABLE II
CALCULATED STATIC PARAMETERS

Symbol	Value	Comment
T_{th}	304.6 K	from Eq. (9b)
n_{th}	$2.6 \cdot 10^{18}$ cm^{-3}	from Eq. (9a)
g_{th}	$8.0 \cdot 10^{12}$ s^{-1}	from Eqs. (9)
g_n'	$3.5 \cdot 10^{-6}$ cm^3/s	from Eq. (12a)
g_T'	$-3.5 \cdot 10^{11}$ meV$^{-1} \cdot$ s^{-1}	from Eq. (12b)
τ_S	1.3 ps	from Eq. (15)
τ_J	8.0 ps	from Eq. (15)
ξ_0	$3.5 \cdot 10^{-18}$ cm^3	from Eq. (18)
γ_S	$1.0 \cdot 10^{-16}$ meV $\cdot$ cm^3	from Eq. (8)
γ_J	$7.7 \cdot 10^{-29}$ meV $\cdot$ cm$^3 \cdot$ s	from Eq. (8)
I_{th}	10.25 mA	$n_{th}/\tau_{sp} \times R_{I:J}$
dP/dI	0.3684 W/A	at threshold
d^2P/dI^2	-0.081 W/A^2	at threshold

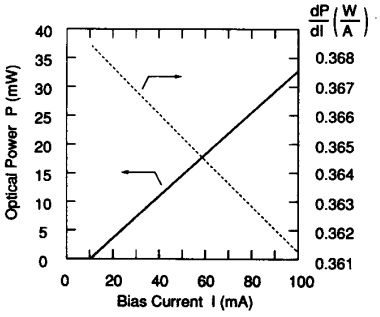

Fig. 2. Calculated static characteristics of the exemplary laser with parameters as in Table I. Variation of the slope efficiency is shown by the broken line.

where

$$\xi_0 \equiv 2\alpha(\tau_S + \tau_J) \approx -g_{\text{th}}^2 \frac{d^2\overline{S}}{d\overline{J}^2}. \tag{18}$$

Note that in the absence of free-carrier absorption ($\alpha = 0$, $\tau_S = 0$), the light-current characteristic is linear in our model, even if there still is carrier heating by the current ($\tau_J \neq 0$). As an increasing $\overline{J}$ heats the carriers, their concentration will rise to compensate the effect of higher $\overline{T}_e$ on the steady-state gain. As evident from (7b), g is constant for $\alpha = 0$.

Calculated parameters of the laser are listed in Table II and the characteristics shown in Fig. 2.

IV. DYNAMIC CHARACTERISTICS

It will be convenient now to change the notation slightly. We shall denote the static values by the subscript 0, and time-dependent terms by an index $i = 1$ or 2, with the increasing refinement of the approximation

$$S = S_0 + S_1 + S_2; \qquad T_e = T_{e0} + T_{e1} + T_{e2};$$

$$n = n_0 + n_1 + n_2. \tag{19}$$

The input current is of the form $J = J_0 + J_1$. The signal $S_1(t)$ is the first-order modulated response of the laser. The pump current signal contains N channels at frequencies $\omega_{K_1} = \omega_0 + K_1 \Delta\omega$, $K_1 = 1, 2, \cdots, N$, viz.,

$$J_1 = \text{Re}\left(\sum_{K_1=1}^{N} a_{K_1} \exp(i\theta_{K_1}) \exp(i\omega_{K_1} t)\right) \equiv \sum_{K_1=1}^{N} \text{Re}\left[J_{K_1} \exp(i\omega_{K_1} t)\right] \tag{20}$$

where $a_{K_1}(t)$ is the (real) modulated amplitude, $J_{K_1} \equiv a_{K_1} \exp(i\theta_{K_1})$, and θ_{K_1} is the phase of K_1th channel signal. In a CSO testing setup, the amplitudes are kept constant, $a_{K_1} \equiv a$, and the optical modulation depth is defined by $a \equiv \mathcal{OMD} \cdot \Delta J_0$. At this point, we make no assumption about the set of $\{\theta_{K_1}\}$; in particular, they may or may not be functions of time.

The second-order variations S_2, n_2 occur at frequencies $\omega_{K_2}^{(\pm)} = |\omega_{K_1} \pm \omega_{M_1}|$, where $K_1, M_1 = 1, 2, \cdots, N$. Because of the equal spacing of the carrier frequencies ω_{K_1}, within each channel the $\omega_{K_2}^{(-)}$ beat appears at $-\delta\omega$ and $\omega_{K_2}^{(+)}$ at $\delta\omega$ relative to the carrier frequency, where $\delta\omega \equiv [\omega_0 \text{ modulo } \Delta\omega]$ (i.e., $\omega_0 \equiv m\,\Delta\omega + \delta\omega$, with m integer). The set of channel numbers $\{K_1, M_1\}$ contributing a second-order beat into a given channel K_2 will be denoted by $[K_2]$ (also the subsets $[K_2^{(+)}]$ and $[K_2^{(-)}]$ contain channel pairs contributing to the sum and the difference beats, respectively.)

Inasmuch as the energy relaxation is much faster (by two to three orders of magnitude) than the characteristic frequencies in the problem, $\tau_\varepsilon \ll \omega^{-1}$, we shall neglect the small frequency dependence of T_e and assume that T_e follow S and J instantaneously

$$T_{ei} = \gamma_S S_i + \gamma_J J_i, \qquad i = 1, 2. \tag{21}$$

Hence,

$$Sg = (S_0 + S_1 + S_2) \times [g_0 + g_n'(n_1 + n_2) + g_T'\gamma_S(S_1 + S_2) + g_T'\gamma_J J_1].$$

Assuming that nonlinear effects are small, $n_2 \ll n_1$ and $S_2 \ll S_1$, we can solve (1) by successive approximations. The zeroth-order equation is given by (16). The first-order equations are of the form

$$(i\omega_{K_1} + \tau_{\text{sp}}^{-1} + \alpha S_0) n_{K_1} + (\Gamma^{-1} i\omega_{K_1} + g_0) S_{K_1} = J_{K_1} \tag{22a}$$

$$n_{K_1} - \left(\frac{i\omega_{K_1}}{\Gamma S_0(g_n' - \alpha)} + \tau_S g_0\right) S_{K_1} = \tau_J J_{K_1}. \quad (22b)$$

The second-order equations are of the form

$$(i\omega_{K_2} + \tau_{sp}^{-1} + \alpha S_0) n_{K_2} + (\Gamma^{-1} i\omega_{K_2} + g_0) S_{K_2} = -\alpha [S_1 \otimes n_1]_{K_2} \quad (23a)$$

$$n_{K_2} - \left(\frac{i\omega_{K_2}}{\Gamma S_0(g_n' - \alpha)} + \tau_s g_0\right) S_{K_2} = \frac{[S_1 \otimes (\tau_J J_1 + \tau_S g_0 S_1 - n_1)]_{K_2}}{S_0}. \quad (23b)$$

The symbols $[X_1 \otimes Y_1]_{K_2}$ are defined in a different way for the sum and the difference beats

$$[X_1 \otimes Y_1]_{K_2}^{(+)} \equiv \frac{1}{4} \sum_{K_1 > M_1}^{[K_2^{(+)}]} (X_{K_1} Y_{M_1} + X_{M_1} Y_{K_1}) \quad (24a)$$

$$[X_1 \otimes Y_1]_{K_2}^{(-)} \equiv \frac{1}{4} \sum_{K_1 > M_1}^{[K_2^{(-)}]} (X_{K_1} Y_{M_1}^* + X_{M_1}^* Y_{K_1}). \quad (24b)$$

Solution of the system of (22) and (23) is straightforward, but the result is, in general, cumbersome. A compact analytic expression obtains if we can neglect compared to unity (but not, of course, compared to terms proportional to τ_S or τ_J) the following terms:

$$\frac{\omega}{\Gamma g_0} \approx \omega \tau_{ph} \quad (25a)$$

$$\frac{\omega^2 \tau_{ph}}{S_0 g_n'} \equiv \frac{\omega^2}{\omega_r^2}; \qquad \frac{\omega \tau_{sp}^{-1} \tau_{ph}}{S_0 g_n'} \equiv \frac{\omega \tau_{sp}^{-1}}{\omega_r^2}. \quad (25b)$$

These approximations are valid sufficiently far from the threshold, at frequencies much less than the resonant frequency of the laser, defined by $2\pi f_r = \omega_r$, where

$$\omega_r^2 \equiv \frac{S_0(g_n' - \alpha)}{\tau_{ph}}. \quad (26)$$

Under the approximation (25) (and also neglecting terms of order $\omega\tau_S$ and $\omega\tau_J$, compared to unity), the determinant of systems (22) and (23) is frequency independent and equals $-g_0$. The first-order equations [(22)] give

$$n_{K_1} \approx J_{K_1} \left(\frac{i\omega_{K_1}}{\omega_r^2} + \tau_S + \tau_J\right) \quad (27a)$$

$$S_{K_1} \approx \frac{J_{K_1}}{g_0}. \quad (27b)$$

From (27) we see that the right-hand sides of (23) contain the following terms:

$$[J_1 \otimes J_1]_{K_2} = \frac{a^2}{2} \Sigma[K_2] \quad (28a)$$

$$[J_1 \otimes i\omega_1 J_1]_{K_2} = \frac{i\omega_{K_2} a^2}{4} \Sigma[K_2] \quad (28b)$$

where the sums $\Sigma[K_2]$ are given by

$$\Sigma[K_2^{(+)}] = \sum_{K_1 > M_1}^{[K_2^{(+)}]} \exp[i(\theta_{K_1} + \theta_{M_1})] \quad (29a)$$

$$\Sigma[K_2^{(-)}] = \sum_{K_1 > M_1}^{[K_2^{(-)}]} \exp[i(\theta_{K_1} - \theta_{M_1})]. \quad (29b)$$

It is remarkable that all terms appearing in the sums (29) are independent of the first-order frequencies that combine in ω_{K_2} and depend only on the phases of the components. Let us trace how this comes about in the instance of (29b) and the difference beat:

$$[J_1 \otimes i\omega_1 J_1]_{K_2}^{(-)} = \frac{1}{4} \sum_{K_1 > M_1}^{[K_2^{(-)}]} J_{K_1}(-i\omega_{M_1}) J_{M_1}^* + J_{M_1}^*(i\omega_{K_1}) J_{K_1} = \frac{i\omega_{K_2}}{4} \sum_{K_1 > M_1}^{[K_2^{(-)}]} J_{K_1} J_{M_1}^* = \frac{i\omega_{K_2} a^2}{4} \Sigma[K_2^{(-)}].$$

Note that this independence on the constituent frequencies would not hold for terms of the form $[n_1 \otimes n_1]_{K_2}$. Such terms appear when the concentration dependence of the carrier lifetime τ_{sp} (e.g., due to Auger processes) is taken into account, cf. the discussion in Section V.

Using (27)–(29) and (23), we find the following approximate expression for the CSO distortion in the presence of carrier heating effects:

$$\frac{|S_{K_2}|}{S_{K_1}} = \frac{\mathcal{OMD}}{4} \left[\left(\frac{\omega_{K_2}^2}{\omega_r^2} + \xi_0 S_0\right)^2 + \left(\frac{\omega_{K_2}}{\omega_r^2 \tau_{sp}}\right)^2\right]^{1/2} |\Sigma[K_2]| \quad (30)$$

where $\xi_0 \equiv 2\alpha(\tau_S + \tau_J)$, as in (18). For frequencies below 600 MHz, as in CATV channels, the difference between the exact solution of (22) and (23) and the approximation (30) is negligible, except very near the threshold.

If the system were designed to control the subcarrier phases, it would be possible to reduce the CSO distortion by a suitable selection of the set $\{\theta_{K_1}\}$; it can be shown, for example, that it is feasible to suppress the sum beats in high-frequency channels at the expense of an enhancement in difference beats which are dominant in low-frequency channels. Minimization of the phase sums (29) seems to be a worthwhile mathematical problem.

In a typical experimental arrangement, the CSO is measured with random phasesθ_{K_1}, generated from a thermal source. Averaging $|\Sigma|$ over the random phases, we find

$$\overline{|\Sigma[K_2^{(+)}]|^2} = \sum_{K_1 > M_1}^{[K_2^{(+)}]} 1 \equiv \mathcal{N}[K_2^{(+)}];$$

$$\overline{|\Sigma[K_2^{(-)}]|^2} = \sum_{K_1 > M_1}^{[K_2^{(-)}]} 1 \equiv \mathcal{N}[K_2^{(-)}]. \quad (31)$$

The number $\mathcal{N}[K_2]$ of channel pairs contributing a CSO distortion in a given channel is plotted in Fig. 3 for an

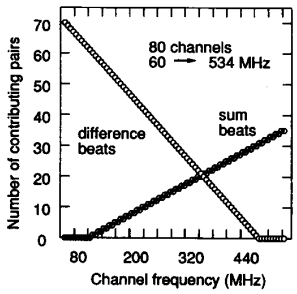

Fig. 3. Number $\mathcal{N}[K_2]$ of contributing channels pairs [equation 31] into a CSO distortion in a given channel, as a function of the channel frequency $2\pi\omega_{K_2}$.

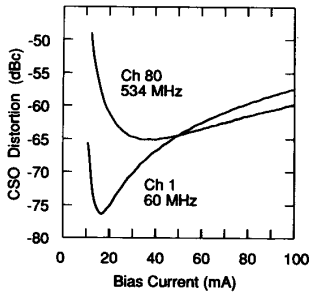

Fig. 4. Composite second-order distortion in a 80-channel analog laser as a function of the pumping current. Laser parameters as in Table I.$\mathcal{OMD} = 3\%$.

80-channel CATV system. The number of pairs $\mathcal{N}[K_2^{(-)}]$ contributing to difference beats decreases linearly from 70 at 60 MHz to 0 in channels with $\omega_{K_2}^{(-)} \geq 480$ MHz. For the sum beats, $\mathcal{N}[K_2^{(+)}]$ increases from 0 for $\omega_{K_2}^{(+)} \leq 120$ MHz to 35 at the high end.

Fig. 4 shows the calculated CSO for an exemplary laser. The CSO is defined by

$$\mathcal{CSO}[\text{dBc}] \equiv 20 \log\left(\frac{|S_{K_2}|}{S_{K_1}}\right).$$

Within the accuracy of the figure, curves obtained by the exact solution of (22) and (23) are indistinguishable from the approximation (30).

Note that at high bias currents, the low-frequency channel (difference beat) has a larger distortion than the high-frequency channel (sum beat), hence the curve crossing in Fig. 4. This phenomenon, often seen experimentally, occurs because the number of contributing channel pairs is twice larger for the low-frequency channel. Increasing current increases the resonant frequency, and in the limit of $\omega_r \to \infty$ the only dependence on the channel frequency is contained in $\mathcal{N}[K_2]$. In this limit, the difference between the two curves tends to 3 dB.

V. Inclusion of the Concentration Dependence of Carrier Lifetime

Equations (22) and (23) and formula (30) were derived under the assumption that the carrier lifetime τ_{sp} is constant. A more accurate description of the differential lifetime [14]

$$\tau_{\text{sp}}^{-1}(n) = A + Bn + Cn^2 \tag{32}$$

introduces an additional nonlinearity directly into the rate equation (1a) for carriers. This leads to a slight modification of our results.

Expanding the terms Bn^2 and Cn^3 according to the scheme (19), we have

$$B(n_0 + n_1 + n_2)^2 = B(n_0^2 + 2n_0n_1 + 2n_0n_2 + n_1^2) \tag{33a}$$

$$C(n_0+n_1+n_2)^3 = C(n_0^3+3n_0^2n_1+3n_0^2n_2+3n_0n_1^2). \tag{33b}$$

Proceeding as in Section IV, we find that the left-hand sides of (22) and (23) retain the same form, except that τ_{sp} is replaced by τ_{eff}, given by

$$\tau_{\text{eff}}^{-1} = A + 2Bn_0 + 3Cn_0^2 \tag{34}$$

and in the right-hand side of (23a) appears an additional term $-(B + 3Cn_0)[n_1 \otimes n_1]_{K_2}$. Using (27a), we can rewrite this term in the form

$$\begin{aligned}[n_1 \otimes n_1]_{K_2} = \frac{1}{\omega_r^4}[i\omega_1 J_1 \otimes i\omega_1 J_1]_{K_2} \\ + \frac{2(\tau_S + \tau_J)}{\omega_r^2}[J_1 \otimes i\omega_1 J_1]_{K_2} \\ + (\tau_S + \tau_J)^2[J_1 \otimes J_1]_{K_2}.\end{aligned} \tag{35}$$

The second line of (35) contains sums of identical terms, independent of the constituent frequencies that produce a beat at ω_{K_2}, cf. (28). In contrast, the sum $[i\omega_1 J_1 \otimes i\omega_1 J_1]_{K_2}$ does not possess this property. Fortunately, the whole term in the first line of (35) is quite negligible. Let us show this in the instance of a sum beat at $\omega_{K_2}^{(+)}$. The largest term in the sum $[i\omega_1 J_1 \otimes i\omega_1 J_1]_{K_2}$ comes from $\omega_{K_1} \approx \omega_{M_1} \approx 1/2\omega_{K_2}$. Therefore, comparing the first and the third terms in the right-hand side of (35), we find that their ratio is less than

$$\frac{1}{4}\frac{\omega_{K_2}^2}{\omega_r^4(\tau_S + \tau_J)^2}$$

which is $\lesssim 3\%$, except very near the threshold. Neglecting the first term, we find a generalized expression for the CSO distortion in the form

$$\frac{|S_{K_2}|}{S_{K_1}} = \frac{\mathcal{OMD}}{4}\left[\left(\frac{\omega_{K_2}^2}{\omega_r^2} + \xi S_0\right)^2 + \left(\frac{\omega_{K_2}}{\omega_r^2 \tau_{\text{eff}}}\right)^2\right]^{1/2} (\mathcal{N}[K_2])^{1/2} \tag{36}$$

where τ_{eff} is given by (34) and the static nonlinearity coefficient ξ by

$$\xi = 2\alpha(\tau_S + \tau_J) + 2g_0(B + 3Cn_0)(\tau_S + \tau_J)^2. \tag{37}$$

Equation (36) is the main result of this paper. For simplicity, it is written for the case when the measured CSO is an average over random phases. Our discussion is general enough to describe the CSO distortion for any distribution of carrier phases, not necessarily random. To treat these situations, one should replace $\sqrt{\mathcal{N}}$ by the phase sum $|\Sigma|$, as in (30).

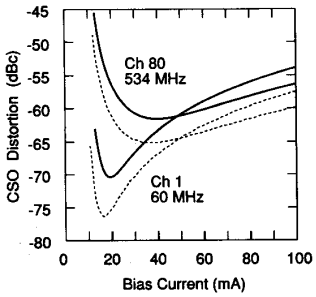

Fig. 5. Composite second-order distortion in an 80-channel analog laser. Laser parameters as in Table I, $\mathcal{OMD} = 3\%$. Carrier lifetime is given by (32) with $B \approx 3.8 \cdot 10^{-10}$ cm^3/s and$C \approx 1.5 \cdot 10^{-28}$ cm^6/s, giving$\tau_{\rm sp}(n_{\rm th}) = 0.5$ ns. The minimum in Ch.80 equals−61.6 dBc and occurs at $I \approx 40$ mA (when $f_r \approx 7$ GHz). For comparison, broken lines show the result at constant $\tau_{\rm sp} = 0.5$ ns (from Fig. 4).

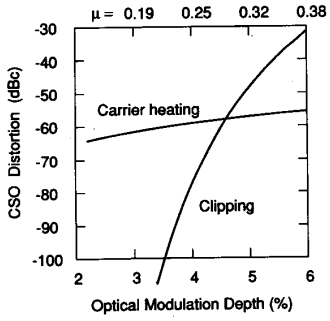

Fig. 6. The OMD dependence of the minimum CSO distortion in Ch.80.Laser parameters as in Fig. 5. The clipping curve, shown for comparison, is calculated according to [9], including only 2nd-order processes and taking the power count $D_\nu^{(2)} = 70$.

Let us compare (36) to the results of Section IV. Take $A = 0$ in (32) and choose B and C so that at threshold both terms contribute the same rate, resulting in $\tau_{\rm sp}(n_{\rm th}) = 0.5$ ns, as in Table I. This corresponds to $B \approx 3.8 \cdot 10^{-10}$ cm^3/s and $C \approx 1.5 \cdot 10^{-28}$ cm^6/s. The calculated CSO distortion is shown in Fig. 5. We see that inclusion of the concentration dependence of $\tau_{\rm sp}$ brings about a tangible correction. This correction occurs for two reasons, both being of comparable importance in our example. First, the static nonlinearity (37) brought about by the dynamic carrier heating effects becomes larger. Inclusion of the concentration dependence of $\tau_{\rm sp}$ raises the value of ξ from $\xi_0 = 3.5 \cdot 10^{-18}$ cm^3 [equation (18)] to $\xi = 5.6 \cdot 10^{-18}$ cm^3. Moreover, ξ no longer depends entirely on the free-carrier absorption: it does not vanish even when $\alpha = 0$. Second, $\tau_{\rm eff}$ resulting from the variable $\tau_{\rm sp}(n)$ is shorter than $\tau_{\rm sp}(n_{\rm th})$; in our example, $\tau_{\rm eff} = 0.2$ ns.

Let us analyze (36) in more detail. It is easy to show that the minimum CSO distortion in a channel of frequency ω_{K_2} equals

$$\left[\frac{|S_{K_2}|}{S_{K_1}}\right]_{\min} = \frac{\mathcal{OMD}\cdot\omega_{K_2}}{2\sqrt{2}} \cdot\left[\frac{\tau_{\rm ph}\xi}{g_n'-\alpha}\left(1+\sqrt{1+(\omega_{K_2}\tau_{\rm eff})^{-2}}\right)\mathcal{N}[K_2]\right]^{1/2} \quad (38)$$

and occurs at the following value of the photon density:

$$S_0^2 = \frac{\omega_{K_2}^2\tau_{\rm ph}\sqrt{1+(\omega_{K_2}\tau_{\rm eff})^{-2}}}{\xi(g_n'-\alpha)}. \quad (39)$$

As evident from (38), an enhancement of the differential gain g_n' by a factor of two decreases the minimum CSO distortion by about 3 dB. Clearly, increasing g_n' is the key strategy for improving CATV lasers.

It is worthwhile to stress that inclusion of the Auger recombination does not imply that we should concern ourselves with a dynamical carrier heating by Auger processes. Such an effect can be described by a term $\sim Cn^2E_G$, added in (1c). The only consequence of this term would be to alter the steady-state carrier temperature—even if the Auger term Cn^2 were the biggest in (32). The effect of Auger heating on the CSO distortion in CATV lasers is negligible, as we have verified by a direct calculation. That this should be the case is evident when we consider that the other heating terms in (1c) are directly proportional to the modulated current, while the Auger term works its dynamics only to the next order of magnitude in ω/ω_r, through the modulation of carrier density. This argument is essentially similar to that above leading to the neglect of the first term in (35).

VI. Comparison to the Clipping Distortion

It is instructive to compare the fundamental limitations on subcarrier multiplexed transmission. Dependence of the minimum CSO distortion in Ch. 80 on the OMD, calculated with (38), is plotted in Fig. 6 together with the corresponding clipping distortion, based on the expression given in [9]. It is clear that for a given number of channels, the clipping distortion [5]–[9] should be dominant at a high enough optical modulation depth, since the CSO due to clipping increases exponentially with OMD, while that due to hot-carrier effects is linear, cf. (36). The characteristic parameter of the clipping distortion, $\mu \equiv \mathcal{OMD}\cdot\sqrt{N/2}$, in the example of Fig. 5 is only $\mu = 0.19$. In this range, the clipping distortion is below −100 dBc for all channels and does not account for the measured values of the CSO distortion [9].

VII. Variations in the Assumed Parameters

With the parameters chosen, (36) predicts a minimum distortion of −61.6 dBc in the high-frequency channel. What variations in the assumed parameters can affect this estimate?

The key coefficient in our model is ξ given by (37). It is determined by the energy relaxation time (mainly by the product $\tau_\varepsilon \cdot \Delta$), the free-carrier absorption coefficient α, and the values of the recombination coefficients B and C. For quantum well lasers, these parameters are not known to a great accuracy. Choosing a different concentration dependence of $\tau_{\rm sp}$ (with the recombination parameters varying over a range of the data in literature [14]), we find a variation in the minimum CSO (Ch.80) of about 3 dB. In our examples, $\tau_J > \tau_S$, i.e., the effect of the heating by current dominates over that due to free-carrier absorption. Inasmuch as the value of τ_J is little affected by a variation in the laser threshold [cf. (15)] and the overall effect of the variable $\tau_{\rm sp}(n)$ [the second term in (37)]

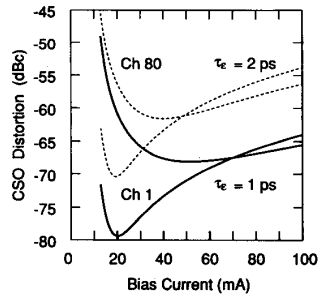

Fig. 7. Composite second-order distortion in an 80-channel laser with parameters as in Fig. 5 and Table I, except $\tau_\varepsilon = 1$ ps. The Ch.80minimum of -65.5 dBc occurs at $I \approx 56$ mA ($f_r \approx 8.7$ GHz). For comparison, broken lines show the results at $\tau_\varepsilon = 2$ ps (from Fig. 5).

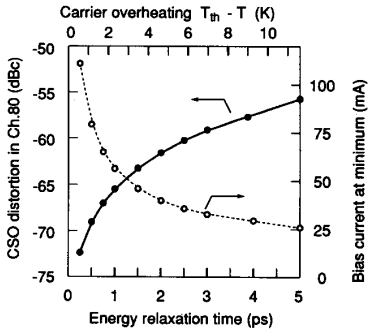

Fig. 8. Dependence of the minimum CSO in Ch.80 on the assumed relaxation time τ_ε. Other laser parameters as in Table I. Broken line shows the bias current corresponding to the CSO minimum. Parameter$T_{\rm th} - T$, from (9b), is indicated on the top horizontal axis.

is scaled by the threshold gain g_0, it is possible to reduce ξ by lowering g_0.

Consider the dependence of our results on the assumed value of the energy relaxation time τ_ε. Fig. 7 shows the CSO distortion calculated with the parameters as in Table I, except for τ_ε which is now taken equal to 1 ps [13]. The dependence $\tau_{\rm sp}(n)$ is included as in Fig. 5. We see that compared to the case of $\tau_\varepsilon = 2$ ps, the minimum CSO distortion decreases (by ~ 4 dB) and the minimum shifts to a higher bias current (~ 56 mA).

The τ_ε dependence of the minimum CSO distortion in the high-frequency channel is plotted in Fig. 8. For a fixed Δ, each assumed value of τ_ε implies a certain carrier overheating $T_{\rm th} - T$ at the threshold, cf. (9b). The experimentally accessible parameter $T_{\rm th} - T$ is indicated in Fig. 8 on a parallel abscissa axis. The amount of overheating is quite modest compared to recent estimates [13]. We believe the actual τ_ε in a QW laser is hardly shorter than 1 ps. Note also that shorter τ_ε would result in the minimum CSO occurring at very high bias currents.

VIII. Conclusion

We have considered nonlinear distortions in a subcarrier multiplexed optical transmission system arising from carrier heating effects in the source laser. We included two sources of the carrier heating: free-carrier absorption of the coherent radiation in the cavity, and the power flux into the active layer, associated with the input current. Resulting from the very existence of modulated optical and electrical signals, these effects cannot be avoided in any laser structure.

We developed an analytical model describing nonlinear dynamics in multichannel single-mode lasers, and obtained simple expressions for the intermodulation distortion on the dc bias level, channel frequency, number of channels, and parameters of the laser. For an 80-channel 60–540 MHz system with 3% optical modulation depth per channel, we find a minimum CSO ≈ -62 dBc in the high-frequency channel. This means that the included fundamental nonlinearities alone account for a distortion near the tolerance limit in CATV systems.

We have also considered another "fundamental" source of carrier heating, resulting from Auger recombination in the active layer. Although important in establishing the steady-state carrier temperature, the Auger heating contributes little nonlinearity and has a negligible effect on the intermodulation distortion.

Acknowledgment

Useful conversations with D. A. Ackerman, N. K. Dutta, M. Haner, A. A. M. Saleh, and L. C. Upadhyayula are gratefully acknowledged.

References

[1] M. Ishino, M. Kito, S. Yamane, K. Fujihara, N. Otsuka, H. Sato, and Y. Matsui, "1.3 μm strained-layer MQW-DFB laser with low noise and low distortion characteristics for 100-channel CATV transmission," in *IEDM'93 Tech. Dig.*, 1993, pp. 613–616.

[2] H. Yonetani, I. Ushijima, T. Takada, and K. Shima, "Transmission characteristics of DFB laser modules for analog applications," *J. Lightwave Technol.*, vol. 11, pp. 147–153, 1993.

[3] U. Cebulla, J. Bouayad, H. Haisch, M. Klenk, G. Laube, H. P. Mayer, R. Weimann, and E. Zielinski, "1.55 μm strained layer multiple quantum well DFB-lasers with low chirp and low distortions for optical analog CATV distribution systems," in *CLEO'93 Tech. Dig.*, vol. 11, 1993, pp. 226–227.

[4] T. E. Darcie, R. S. Tucker, and G. J. Sullivan, "Intermodulation and harmonic distortion in InGaAsP lasers," *Electron. Lett.*, vol. 21, pp. 665–666, 1985.

[5] A. A. M. Saleh, "Fundamental limit on number of channels in subcarrier-multiplexed lightwave CATV system," *Electron. Lett.*, vol. 21, pp. 776–777, 1989.

[6] T. E. Darcie, "Subcarrier multiplexing for lightwave networks and video distribution systems," *IEEE J. Select. Areas Commun.*, vol. 8, pp. 1240–1248, 1990.

[7] K. Alameh and R. A. Minasian, "Ultimate limits of subcarrier multiplexed transmission," *Electron. Lett.*, vol. 27, pp. 1260–1262, 1991.

[8] Q. Shi, R. S. Burroughs, and D. Lewis, "An alternative model for laser clipping-induced nonlinear distortion for analog lightwave CATV systems," *IEEE Photon. Technol. Lett.*, vol. 4, pp. 784–787, 1992.

[9] N. J. Frigo, M. R. Phillips, and G. E. Bodeep, "Clipping distortion in lightwave CATV systems: models, simulations, and measurements," *J. Lightwave Technol.*, vol. 11, pp. 138–146, 1993.

[10] H. Kawamura, K. Kamite, H. Yonetani, S. Ogita, H. Soda, and H. Ishikawa, "Effect of varying threshold gain on second-order intermodulation distortion in distributed feedback lasers," *Electron. Lett.*, vol. 26, pp. 1720–1721, 1990.

[11] C. H. Henry, R. A. Logan, F. R. Merritt, and J. P. Luongo, "The effect of intervalence band absorption on the thermal behavior of InGaAsP lasers," *IEEE J. Quantum Electron.*, vol. QE-19, pp. 947–952, 1983.

[12] C. Y. Tsai, L. F. Eastman, and Y. H. Lo, "Hot carrier and hot phonon effects on high-speed quantum well lasers," *Appl. Phys. Lett.*, vol. 63, pp. 3408–3410, 1993.

[13] K. L. Hall, G. Lenz, E. P. Ippen, U. Koren, and G. Raybon, "Carrier heating and spectral hole burning in strained-layer quantum-well laser amplifiers at 1.5 μm," *Appl. Phys. Lett.*, vol. 61, pp. 2512–2514, 1992.
[14] G. P. Agrawal and N. K. Dutta, *Semiconductor Lasers*, 2d ed. New York: Van Nostrand Reinhold, 1993, p. 124.

V. B. Gorfinkel received her Ph.D. degree in semiconductor physics in 1980 from the Ioffe Physico-Technical Institute, St. Petersburg, Russia. Until 1991 she had worked at the Institute for Radioelectronics, USSR Academy of Sciences. Since 1991 she has been with the University of Kassel, Germany. Her main research interests are in the physics of exploratory high-frequency semiconductor optoelectronic devices.

S. Luryi (M'81–SM'85–F'90) received his Ph.D. degree in physics from the University of Toronto in 1978. Between 1980 and 1994 he was a member of technical staff at AT&T Bell Laboratories in Murray Hill, NJ. During this period he served as a group supervisor in several device research departments, dealing with VLSI, quantum phenomena, and optoelectronics. He has published over 130 papers and filed 26 US patents in the areas of high-speed electronic and photonic devices, material science, and advanced packaging. In 1990 Bell Laboratories recognized him with the Distinguished Member of Technical Staff award. During 1986–1990 Dr. Luryi served on the Editorial Board of the *IEEE Transactions on Electron Devices,* first as an Associate Editor and then the Editor. In 1989 Dr. Luryi was elected Fellow of the IEEE "for contributions in the field of heterojunction devices" and in 1993 Fellow of the American Physical Society "for theory of electron transport in low-dimensional systems and invention of novel electron devices." In 1994 Dr. Luryi joined the faculty of the State University of New York at Stony Brook where is currently a leading professor and Chairman of the Department of Electrical Engineering.